

Manuscript version: Author's Accepted Manuscript

The version presented in WRAP is the author's accepted manuscript and may differ from the published version or Version of Record.

Persistent WRAP URL:

<http://wrap.warwick.ac.uk/120677>

How to cite:

Please refer to published version for the most recent bibliographic citation information. If a published version is known of, the repository item page linked to above, will contain details on accessing it.

Copyright and reuse:

The Warwick Research Archive Portal (WRAP) makes this work by researchers of the University of Warwick available open access under the following conditions.

Copyright © and all moral rights to the version of the paper presented here belong to the individual author(s) and/or other copyright owners. To the extent reasonable and practicable the material made available in WRAP has been checked for eligibility before being made available.

Copies of full items can be used for personal research or study, educational, or not-for-profit purposes without prior permission or charge. Provided that the authors, title and full bibliographic details are credited, a hyperlink and/or URL is given for the original metadata page and the content is not changed in any way.

Publisher's statement:

Please refer to the repository item page, publisher's statement section, for further information.

For more information, please contact the WRAP Team at: wrap@warwick.ac.uk.

A Synthetically Scalable Poly(ampholyte) which Dramatically Enhances Cellular Cryopreservation

Trisha L. Bailey,^a Christopher Stubbs,^a Kathryn Murray,^a Ruben M. F. Tomás,^a Lucienne
Otten,^a Matthew I. Gibson^{a,b,*}

^a) Department of Chemistry, University of Warwick, Coventry, CV4 7AL, United Kingdom

^b) Warwick Medical School, University of Warwick, Coventry, CV4 7AL, United Kingdom

CORRESPONDING AUTHOR DETAILS

*Fax: +44 247 652 4112. E-mail: m.i.gibson@warwick.ac.uk

Abstract

The storage and transport of frozen cells underpins emerging/existing cell-based therapies and is used in every biomedical research lab globally. The current gold-standard cryoprotectant (DMSO) does not give quantitative cell recovery in suspension nor in 2D or 3D cell models and the solvent and cell debris must be removed prior to application/transfusion. There is a real need to improve this 50 year old method to underpin emerging regenerative and cell-based therapies. Here we introduce a potent and synthetically scalable polymeric cryopreservation enhancer which is easily obtained in a single step from the low cost and biocompatible precursor poly(methyl vinyl ether-*alt*-maleic anhydride). This polyampholyte enables post-thaw recoveries of up to 88 % for a 2-D cell monolayer model compared to just 24 % using conventional DMSO cryopreservation. The polyampholyte also enables reduction of [DMSO] from 10 wt % to just 2.5 wt % in suspension cryopreservation, which can reduce the negative side-effects and speed up post-thaw processing. Post-thaw, the cells have reduced membrane damage and faster growth rates compared to those without the polymer. The polymer appears to function by a unique extracellular mechanism, by stabilisation of the cell membrane, rather than by modulation of ice formation and growth. This new macromolecular cryoprotectant will find applications across basic and translational biomedical science and may improve the cold-chain for cell-based therapies.

Introduction

Cryopreservation is an essential process for the long-term storage of cells and tissues. Red blood cells are the most frequently transfused blood product, with 12–16 million units transfused per year in the United States alone,¹ but difficult processing has shifted the use of cryopreserved RBCs to settings only where their availability is limited.² Leukaemia therapy is underpinned by the transfusion of (DMSO) cryopreserved hematopoietic stem cells, and mammalian cells are widely used in the biopharmaceutical industry for the production of recombinant therapeutic proteins (biologics).³ However, it is not currently possible or practical to supply this material reproducibly due to phenotypic changes of growing cultures, therefore the banking of these materials is essential.⁴ Additionally, the ability to preserve cells as monolayers, which can be readily used and do not need to be propagated forward, would be revolutionary in providing identical starting materials, for instance, ensuring precisely engineered reporter lines do not experience any sort of propagated “phenotypic drift” which would alter their precise reporting mechanisms.⁵ Furthermore, there is evidence that the core response of cells to cryopreservation is different if the cells are part of a network and the scale-up of procedures from a microscopic cellular level to a macroscopic tissue scale will introduce new modes of injury specific to tissue freezing.⁶ Our monolayer results could pave the way to improve organ-on-a-chip preservation outcomes⁷ or perhaps even be the key to successful tissue preservation.

The gold standard protocol for the (suspension) cryopreservation of mammalian cells is vial freezing in a solution containing 5-10 % of the cryoprotective agent (CPA) dimethyl sulfoxide (DMSO), which is able to enter cells and partly reduce injury by moderating the increase of solute concentration during freezing.⁸⁻¹⁰ Additionally, cells frozen in vials must be propagated forward through several passages before they are stable enough to be used for reproducible assays. While vial freezing in DMSO works for most cell lines, many are highly-sensitive to

DMSO.¹¹ The ability to reliably store all cells and to employ lower concentrations of DMSO would aid multiple fields by increasing post-thaw viability and reducing processing. Compared to freezing in solution, DMSO does not work well for cell monolayers,¹² typically resulting in only around 20 – 35 % cell recovery.^{13,14} Clearly, there exists a real need to transform our approach to cryopreservation, in order to boost cell recovery, function, and reduce the processing challenges.

Despite the above cryopreservation challenges, extremophiles have evolved in nature to allow survival at sub-zero conditions by both promoting and/or inhibiting the formation and growth of ice, presenting major opportunities for biomedicine. In addition to these strategies, extremophiles use the production of osmotic protectants such as trehalose,^{15–17} proline,^{18–21} and sucrose,²² as well as macromolecules such as antifreeze proteins,^{23,24} or late embryogenesis abundant proteins (LEAs).²⁵ Synthetic polymers, which mimic antifreeze proteins' ice recrystallisation inhibition (IRI) properties, have emerged in recent years as promising cryoprotectants.^{26–28} Ice recrystallisation during thawing is a major cause of cell death, and IRI active polymers such as poly(vinyl alcohol) can lead to increases in post-thaw yield.²⁹ Poly(proline), which displays moderate IRI, has been shown to improve post-thaw recovery of cell monolayers, potentially by interacting with cell membranes as well as its IRI.³⁰ These examples show that macromolecular cryoprotectants can be designed to modulate membrane stability as well as ice growth, presenting an exciting opportunity. Carboxylated poly(lysine), and other synthetic poly(ampholytes) bearing mixed positive and negative charges can interact with cell membranes and have been evaluated in cryovial vitrification³¹, monolayer slow-vitrification³², or slow-freezing in cryovials³³ but never slow-freezing of monolayers. These result in good post-thaw recoveries but require, for example, 6.5M ethylene glycol solutions and often very fast cooling rates,³² as well as the issue of removing such a high concentration of solvent from the cells before toxicity occurs. They are also not synthesised on a large scale,

necessary for a step-change in how cryopreservation is conducted, and hence they have not been widely adopted.

Despite the above progress, the actual cell yields obtained with poly(ampholytes) can still be low, and often require vitrification (formation of an ice-free state using very high solvent loads), which is not typically practical for most cellular cryopreservation settings. An ideal polymeric cryoprotectant would increase cell yield post-thaw, be easily removed, available on a commercial scale for wide use, enable monolayer as well as suspension cell cryopreservation, and enhance the cryopreservation of all cell types with minimal re-formulation requirements. Here we report a poly(ampholyte) cryopreservative that significantly enhances the post-thaw cell yield of a broad range of cell types including nucleated and anucleated cells in suspension and as monolayers under slow freezing conditions. The polymer is easily obtained from a clinically used, low cost, precursor which ensures scalability. Additionally, it appears that the polymer externally protects cell membranes during freezing as its main mode of action, rather than ice growth modulation, and since it does not enter the cells, it is easily removed. We also demonstrate that the DMSO concentration required can be reduced as low as 2.5 wt % through the use of a higher concentration of polymer.

Methods and Materials

Materials. Phosphate-buffered saline (PBS) solutions were prepared using pre-formulated tablets (Sigma-Aldrich) in 200 mL of Milli-Q water ($>18.2 \Omega$ mean resistivity) to give $[\text{NaCl}] = 0.138 \text{ M}$, $[\text{KCl}] = 0.0027 \text{ M}$, and pH 7.4. Poly(methyl vinyl ether-alt-maleic anhydride) M_n 80,000 and 311,000 $\text{g}\cdot\text{mol}^{-1}$, dimethylaminoethanol and *N*-[4-(aminomethyl)benzyl]rhodamine 6G-amide bis(trifluoroacetate) were purchased from Sigma-Aldrich. Poly(methyl vinyl ether-alt-maleic anhydride) average M_n 20,000 $\text{g}\cdot\text{mol}^{-1}$ was purchased from Scientific Polymer Products, the dispersity of polymer **P2** from the manufacturer is 2.7, **P3** is 3.47; the supplier of **P1** does not list the M_w value, only the M_n . Sodium chloride was purchased from Fisher Scientific. All solvents were purchased from VWR or Sigma Aldrich and reagents were used without further purification unless indicated.

Note on the choice of polymer: Dimethylamino functionality was selected for the cationic component. This was driven by our previous observations on the role of hydrophobicity on ice crystal growth, that ethyl and propyl modifications gave lower activity.³⁴ Secondly, there were solubility reasons; When more hydrophobic pendant groups are installed [diethyl and diisopropyl] dissolution becomes an issue, with these samples having limited solubility at concentrations greater than 20 $\text{mg}\cdot\text{mL}^{-1}$. For these polymers to be practical in a lab, concentrations stocks need to be made, meaning that concentrations of at least 2 x what is required for cryopreservation must be achieved. The dimethyl amino gave this balance.

Synthesis of Polyampholytes. As a representative example, poly(methyl vinyl ether-*alt*-maleic anhydride), average $M_n \sim 80,000 \text{ Da}$, (1 g) was dissolved in tetrahydrofuran (50 mL) and heated to 50 °C with stirring. After dissolution, dimethylamino ethanol (2 g) was added in excess, forming a pink waxy solid, which was allowed to stir for 30 minutes. 50 mL water was added, and the reaction left to stir overnight followed by purification in dialysis tubing (Spectrapor, 12 – 14 kDa MWCO) for 48 hours with 7 water changes. The resulting solution was freeze-dried to evolve a white solid.

^1H NMR (DMSO): $\delta = 2.30 - 2.80$ ($\text{CH}_2\text{CH}(\text{OCH}_3)\text{CH}_2$, br), 2.42 ($(\text{CH}_3)_2\text{NCH}_2$, s, 6H), 2.50 ($\text{CH}_2\text{CH}(\text{OCH}_3)\text{CH}_2$, s, 3H), 2.66 ($\text{NCH}_2\text{CH}_2\text{COO}$, t, 2H), 3.02 – 3.37 ($\text{CH}_2\text{CH}(\text{OCH}_3)\text{CH}_2$), 3.41 – 4.48 ($\text{CH}(\text{OCH}_3)\text{CH}(\text{COOH})\text{CH}(\text{COOC})$, $\text{CH}(\text{OCH}_3)\text{CH}(\text{COOH})\text{CH}(\text{COOC})$, br), 3.56 ($\text{NCH}_2\text{CH}_2\text{COO}$, t, 2H). ^{13}C NMR (DMSO): 42 ($(\text{CH}_3)_2\text{NCH}_2$), 55 ($\text{NCH}_2\text{CH}_2\text{COO}$), 58

(NCH₂CH₂COO). IR: 1220 cm⁻¹ (C-O), 1342 (C-N), 1560 (O=C-O⁻ Carboxylate), 1724 (C=O), 2364 (Me₂N-H⁺ ammonium).

Synthesis of Fluorescently Labelled Polyampholytes. As a representative example, poly(methyl vinyl ether-*alt*-maleic anhydride), average M_n ~80,000 Da, (300 mg) was dissolved in tetrahydrofuran (50 mL) and heated to 50 °C with stirring. After dissolution, *N*-[4-(aminomethyl)benzyl]rhodamine 6G-amide bis(trifluoroacetate) (3 mg) and triethylamine (10 mg) were added and left for 20 minutes before dimethylamino ethanol (2 g) was added in excess, forming a pink waxy solid, which was allowed to stir for 30 minutes. 50 mL water was added, and the reaction left to stir overnight followed by purification in dialysis tubing (Spectrapor, 12 – 14 kDa MWCO) for 48 hours with 7 water changes. The resulting solution was freeze-dried to evolve a white solid.

Physical and Analytical Methods. ¹H and ¹³C NMR spectra were recorded on Bruker Avance III HD 300 MHz, HD 400 MHz or HD 500 MHz spectrometers using deuterated solvents obtained from Sigma-Aldrich. Chemical shifts are reported relative to residual non-deuterated solvent.

Ice Recrystallisation Inhibition Assay. Ice wafers were annealed on a Linkam Biological Cryostage BCS196 with T95-Linkpad system controller equipped with a LNP95-Liquid nitrogen cooling pump, using liquid nitrogen as the coolant (Linkam Scientific Instruments UK, Surrey, UK). An Olympus CX41 microscope equipped with a UIS-2 20x/0.45/∞/0-2/FN22 lens (Olympus Ltd, Southend on sea, UK) and a Canon EOS 500D SLR digital camera was used to obtain all images. Image processing was conducted using Image J, which is freely available from <http://imagej.nih.gov/ij/>. LogP was calculated from the hydrophobicity of the pendant group using ChemDraw Professional 16.0.

IRI evaluation. A 10 μL droplet of polymer in PBS solution was dropped from 1.4 m onto a glass microscope coverslip, on top of an aluminium plate cooled to -78 °C using dry ice. The droplet freezes instantly upon impact with the plate, spreading out and forming a thin wafer of ice. This wafer was then placed on a liquid nitrogen cooled cryostage held at -8 °C. The wafer was then left to anneal for 30 minutes at -8 °C. The number of crystals in the image were counted, again using ImageJ, and the area of the field of view divided by this number of crystals

to give the average crystal size per wafer, and reported as a percentage of area compared to PBS control.

Differential scanning calorimetry (DSC). Samples were prepared by weighing standard 40 μL aluminium pans and lids (Mettler Toledo, Leicestershire, UK) and adding 20 μL of solution before hermetically sealing and reweighing in order to quantify the exact mass of sample. Each sample was then transferred to a liquid nitrogen cooled DSC 1 STAR® system (Mettler Toledo) differential scanning calorimeter. The mass of the aluminium pan and sample mass was input into the complimentary STARe thermal analysis software to retain a digital record and aid analysis.

Freezing and thawing of DSC samples and evaluation of DSC spectra. Each DSC sample was individually cooled from +25 °C to -150 °C at a rate of 10 °C.min⁻¹ while concurrently monitoring the heat flow (mW) of the system to detect any endothermic or exothermic transitions. When samples reached -150 °C, each sample was held for 10 min, then warmed at a rate of 10 °C.min⁻¹ from -150 °C to +25 °C.

Blood Testing Protocol. 10 mL Sheep blood in Alsevers solution was added to a 15 mL centrifuge tube and centrifuged at 2000 rpm for 5 m to concentrate the solution, 7 mL of the supernatant was removed and replaced with 7 mL PBS solution. Polymer solutions were made at 2X the required concentration to ensure the correct final cryoprotectant concentration. 0.5 mL of the blood solution was added to 0.5 mL of the polymer solutions in 2 mL cryovials. These were then incubated in the fridge for 30 m before freezing above liquid nitrogen vapour. After 1 h, samples were thawed in a water bath at 45 °C for 10 m, after which they were transferred to Eppendorf tubes and centrifuged at 2000 rpm for 5 m. 40 μL of the supernatant was removed and added to 750 μL of AHD solution. After vortexing, the samples were pipetted into a 96 well plate in triplicate (3 x 200 μL per sample) and the absorbance recorded at 580nm in the BioTek plate reader. Samples were compared against unfrozen PBS and lysis buffer samples as the 0 and 100% lysis samples respectively.

Cell Culture. Human Caucasian lung carcinoma cells (A549) were obtained from European Collection of Authenticated Cell Cultures (ECACC) (Salisbury, UK) and grown in 175 cm² cell culture Nunc flasks (Corning Incorporated, Corning, NY). Standard cell culture medium was composed of Ham's F-12K (Kaighn's) Medium (F-12K) (Gibco, Paisley, UK)

supplemented with 10% USA-origin fetal bovine serum (FBS) purchased from Sigma Aldrich (Dorset, UK), 100 units·mL⁻¹ penicillin, 100 µg·mL⁻¹ streptomycin, and 250 ng·mL⁻¹ amphotericin B (PSA) (HyClone, Cramlington, UK). Mouse calvarial osteoblastic cells (MC-3T3) were obtained from ECACC and grown in 75 cm² cell culture Nunc flasks. Standard cell culture medium was composed of Minimum Essential Medium α (Gibco) supplemented with 10% USA-origin fetal bovine serum (FBS), 100 units·mL⁻¹ penicillin, 100 µg·mL⁻¹ streptomycin, and 250 ng·mL⁻¹ amphotericin B (PSA). Mouse brain neuroblastoma cells (Neuro-2a) were obtained from American Tissue Culture Collection (ATCC) (Middlesex, UK) and grown in 75 cm² cell culture Nunc flasks. Standard cell culture medium was composed of Eagle's Minimum Essential Media (EMEM) (Gibco) supplemented with 10% USA-origin fetal bovine serum (FBS), 100 units·mL⁻¹ penicillin, 100 µg·mL⁻¹ streptomycin, and 250 ng·mL⁻¹ amphotericin B (PSA). All cells were maintained in a humidified atmosphere of 5% CO₂ and 95% air at 37 °C and the culture medium was renewed every 3–4 days. The cells were subcultured every 7 days or before reaching 90% confluency. To subculture, cells were dissociated using 0.25% trypsin plus 1 mM EDTA in balanced salt solution (Gibco). A549 cells were reseeded at 1.87·10⁵ cells per 175 cm² cell culture flasks. MC-3T3 cells were reseeded at 1.87·10⁵ cells per 75 cm² cell culture flasks. Neuro-2a cells were reseeded at 7.5·10⁴ per 75 cm² cell culture flasks.

Cell Solution Preparation. Solutions for cell incubation experiments were prepared by dissolving the individual compounds in base cell media supplemented with 10% FBS and 1x PSA (solutions used as freezing buffers did not contain PSA) and sterile filtered prior to use.

Cytotoxicity Screening.

Polyampholyte cytotoxicity. A549 cells were seeded at 4·10⁴ cells per well in 200 µL of cell culture medium with indicated concentrations of polyampholyte in 96-well plates (ThermoFisher). Cells were incubated with polymer for 10 m and exchanged against completed cell media or incubated with polymer for 24 h in a humidified atmosphere of 5% CO₂ and 95% air at 37 °C. Following the incubation period, resazurin sodium salt (Sigma Aldrich) was dissolved in phosphate buffered saline (PBS) (Sigma Aldrich) and added to wells in an amount of 1/10th initial well volume. Readings were taken using the Synergy HTX Multi-Mode Reader (BioTek, Swindon, UK) at 570/600 nm absorbance every 30 m until control cells reached ~70% reduction.

DMSO cytotoxicity. A549 cells were seeded at $1 \cdot 10^4$ cells per well in 100 μL of cell culture medium with indicated concentrations of DMSO in 96-well plates. Cells were incubated for 30 m in a humidified atmosphere of 5% CO_2 and 95% air at 37 $^\circ\text{C}$. After 30 m the media was exchanged for fresh cell media and a resazurin sodium salt assay was performed as described previously. Values were normalized by dividing experimental values by control values

Membrane Kinetics. Methods adapted from Su³⁵. A549 cells were dissociated and incubated with 1 μM of calcein-AM (BD Biosciences, Workingham, UK) in completed cell media for 30 m at 37 $^\circ\text{C}$ with frequent mixing. Cells were then centrifuged and rinsed twice with media. Cells were plated at a density of $4 \cdot 10^5$ in 100 μL in 96-U-well suspension plates (Sarstedt Ltd., Leicester, UK) and centrifuged at 500 rpm for 2 m. Experimental solutions of 50 μL were added at 4x and 50 μL of 0.32% trypan blue was added for a final concentration of 0.08%. Plate was placed in the BioTek plate reader at 37 $^\circ\text{C}$ and read every 10 m at 494/517 nm for 4 h. Plate was then imaged with the CKX41 microscope with LED illumination, the XC30 camera, and processed using the CellSens software.

Live/Dead Staining of Polyampholyte Incubation. A549 cells seeded at $4 \cdot 10^5$ cells per well in 500 μL of cell culture medium in 24-well plates. Cells were incubated with polymer for 24 h in a humidified atmosphere of 5% CO_2 and 95% air at 37 $^\circ\text{C}$. Following the 24 h incubation, cells were incubated with 0.3 μM calcein (ThermoFisher) and 10 μM ethidium homodimer-1 (ThermoFisher) in PBS. Cells were incubated at room temperature for 45 m. Stain solution was removed and wells were washed twice with PBS. Plate was read using the BioTex plate reader at 494/517 nm and 528/617 nm. Plate was then imaged with the CKX41 microscope with pE-300-W LED illumination, the XC30 camera, and processed using the CellSens software.

Cryopreservation of Cell Suspensions. A549 cells for suspension freezing were removed from adherent culture by treatment with 0.25% trypsin plus 1 mM EDTA in balanced salt solution for 5 m in a humidified atmosphere of 5% CO_2 and 95% air at 37 $^\circ\text{C}$. The number of viable cells was determined by counting with a hemocytometer (Sigma Aldrich) at room temperature after 1:1 dilution of the sample with 0.4% trypan blue solution (Sigma Aldrich). The cell density was adjusted to obtain a cell suspension of $1 \cdot 10^5$ cells $\cdot\text{mL}^{-1}$. Solutions containing the poly(ampholyte) were prepared at 2X the final concentration in F12-K media

containing 20% FBS and 2X the indicated concentration of dimethyl sulfoxide (DMSO). 500 μ L cell suspension and 500 μ L freezing solution was added to individual cryovials (2 mL, Nalgene®, Thermo Scientific, NY) and mixed three times with a 1000 μ L pipette. Final concentration of FBS in freezing solutions was 10%. Cryovials were placed in a CoolCell® LX freezing container (BioCision, LLC, Larkspur, CA), and transferred to a -80 °C freezer where they were frozen at a rate of 1 °C·min⁻¹. After 2 h at -80 °C, vials were transferred to the vapour phase of a liquid nitrogen dewar at -196 °C for 24 h. After 24 h at -196 °C, cells were rapidly thawed by placing the vials in a foam support in a water bath set to 37 °C. The contents of each vial were added to 9 mL complete F-12K media and centrifuged at 2 g for 5 m to pellet cells. The supernatant was discarded and the cell pellet was resuspended in 500 μ L complete cell media then transferred to individual wells of a 24-well plate (Corning Incorporated, Corning, NY). Cells were placed in a humidified atmosphere for 24 h and then dissociated using 0.25% trypsin plus 1 mM EDTA in balanced salt solution. The number of viable cells was then determined by counting with a hemocytometer at room temperature after 1:1 dilution of the sample with 0.4% trypan blue solution. The initial cell medium was discarded such that any non-attached cells were not included in the assessment. The percentage of recovered cells was calculated by dividing the number of cells with intact membranes after freezing and thawing by the number of cells initially frozen, multiplied by 100.

Cryopreservation of Cell Monolayers. Methods adapted from Bailey¹⁴. A549 cells to be frozen in the monolayer format were seeded at $4 \cdot 10^5$ cells per well in 500 μ L of cell culture medium in 24-well plates. MC-3T3 and Neuro-2a cells to be frozen in the monolayer format were seeded at $5 \cdot 10^5$ cells per well in 500 μ L of cell culture medium in 24-well plates (Neuro-2a cells were frozen on collagen coated plates). Plates had a total available volume of 3.4 mL with an approximate growth area of 1.9 cm², no coverslips were used and plates were used with the accompanying lid. Cells were allowed to attach to the entire free surface of the bottom of the well and formed a confluent layer not greater in height than one cell. Before experimental treatments, cells were allowed to attach for 2 h to the plates in a humidified atmosphere of 5% CO₂ and 95% air at 37 °C. The medium was exchanged against fresh medium to remove all unattached cells and then incubated for 24 h in a humidified atmosphere of 5% CO₂ and 95% air at 37 °C. Following the incubation period, the culture medium was removed and cells were exposed for 10 m at room temperature to different concentrations of solutes dissolved in base media supplemented with 10% FBS and the indicated concentrations of dimethyl sulfoxide (DMSO). After 10 min, the freezing solutions were removed and the plate placed inside a

CoolCell® MP plate (BioCision), transferred to a -80 °C freezer and frozen at a rate of 1 °C·min⁻¹. After 24 h at -80 °C, cells were rapidly thawed by addition of 500 µL cell culture medium warmed to 37 °C. Cells were placed in a humidified atmosphere for 24 h and then dissociated using 0.25% trypsin plus 1 mM EDTA in balanced salt solution. The number of viable cells was then determined by counting with a hemocytometer at room temperature after 1:1 dilution of the sample with 0.4% trypan blue solution. The initial cell medium was discarded such that any non-attached cells were not included in the assessment. The percentage of recovered cells was calculated by dividing the number of cells with intact membranes after freezing and thawing by the number of cells present prior to freezing (i.e. after application of pre-treatments), multiplied by 100.

Collagen plate coating. Collagen I from rat tail (Sigma-Aldrich) was diluted to 50 µg·mL⁻¹ in 200 mM acetic acid (Sigma) and added to each well of the cell culture plate at 5 µg collagen·cm⁻². Plates were incubated with the dissolved collagen for 1 h and after this incubation period the collagen solution was removed and the plates were rinsed three times with 200 µL PBS to remove any residual acetic acid solution. The collagen treated plates were allowed to dry for 1 h in a laminar flow hood and stored for less than 1 week at 4 °C prior to use.

Post-Freeze Viability. A549 cells were cryopreserved as previously indicated. After dissociation and counting, cells were plated at a density of $1.25 \cdot 10^4$ per well in a 6-well plate (ThermoFisher). For low yield recovery, multiple freezing wells were combined to provide an adequate number of cells. Control cells were plated at the same density with no prior manipulation. Cells were incubated in a humidified atmosphere of 5% CO₂ and 95% air at 37 °C for the indicated number of days and then dissociated using 0.25% trypsin plus 1 mM EDTA in balanced salt solution for counting. Cell media was replaced on day four with fresh media. Growth rates were calculated by dividing the number of cells present by the initial plating density.

Post-Freeze Membrane Permeability. A549 cells were cryopreserved as previously indicated. Following the 24 h post-thaw incubation, cells were incubated with 0.3 µM calcein and 10 µM ethidium homodimer-1 in PBS. Cells were incubated at room temperature for 45 min. Stain solution was removed and wells were washed twice with PBS. Plate was read using the BioTex plate reader at 494/517 nm and 528/617 nm. Plate was then imaged with the CKX41 microscope with pE-300-W LED illumination, the XC30 camera, and processed using the CellSens software.

Statistical Analyses. Data were analysed with a one-way analysis of variance (ANOVA) on ranks followed by comparison of experimental groups with the appropriate control group (Holm–Sidak method) followed by Tukey’s post hoc test. Excel 2013 (Microsoft, Redmond, WA) and R (R Foundation for Statistical Computing, Vienna, Austria) were used for the analyses and graphs. Data sets are presented as mean \pm (SEM).

Results

Poly(methyl vinyl ether-*alt*-maleic anhydride) $M_n = 20$ kDa (**P1**), 80 kDa (**P2**), and 311 kDa (**P3**) was selected as the precursor to a poly(ampholyte) as it is produced on multi-ton scales, and is safe as both a food additive and bio-adhesive.³⁶ The anhydride was ring-opened by addition of dimethylamino ethanol to give a poly(ampholyte) of appropriate hydrophobicity and solubility³⁴ (Figure 1a, characterization data shown in Figure S1). Other, more hydrophobic, amine substituents result in less soluble materials and the dimethyl was found in screening to provide the best balance. By using an anhydride precursor we guarantee the 1:1 ratio of cationic/anionic groups and regioregularity, not obtainable by other co-polymerization methods. Ice recrystallisation inhibition (IRI) assays³⁷ (where smaller ice crystals indicate more activity) showed that **P1-P3** had only weak, molecular weight dependant, IRI activity (Figure 1b), below that of other poly(ampholytes).^{34,38} For reference, type I antifreeze protein, used as a positive control, leads to < 20 % mean grain size at < 1 mg.mL⁻¹ concentrations (Figure S2) and hence the poly(ampholytes) can be considered to be very weakly IRI active when discussing mechanisms of cryopreservation (below). DSC (differential scanning calorimetry) confirmed ice crystallisation in the presence of **P2**, thus ruling out non-colligative effects. The small differences in the enthalpy of crystallisation are what we would expect due to solute concentration effects on freezing point depression³⁹, and showing vitrification (an entirely different cryopreservation approach where a glass is formed instead of ice^{31,32}) is not occurring

(Figure 1c). Full DSC traces and onset melting temperatures are shown in Figure S3 and S4 respectively. As there is only weak IRI activity, any emergent cryoprotectant properties (*vide infra*) can be correlated to unique cellular interactions, such as with the cell membrane.⁴⁰

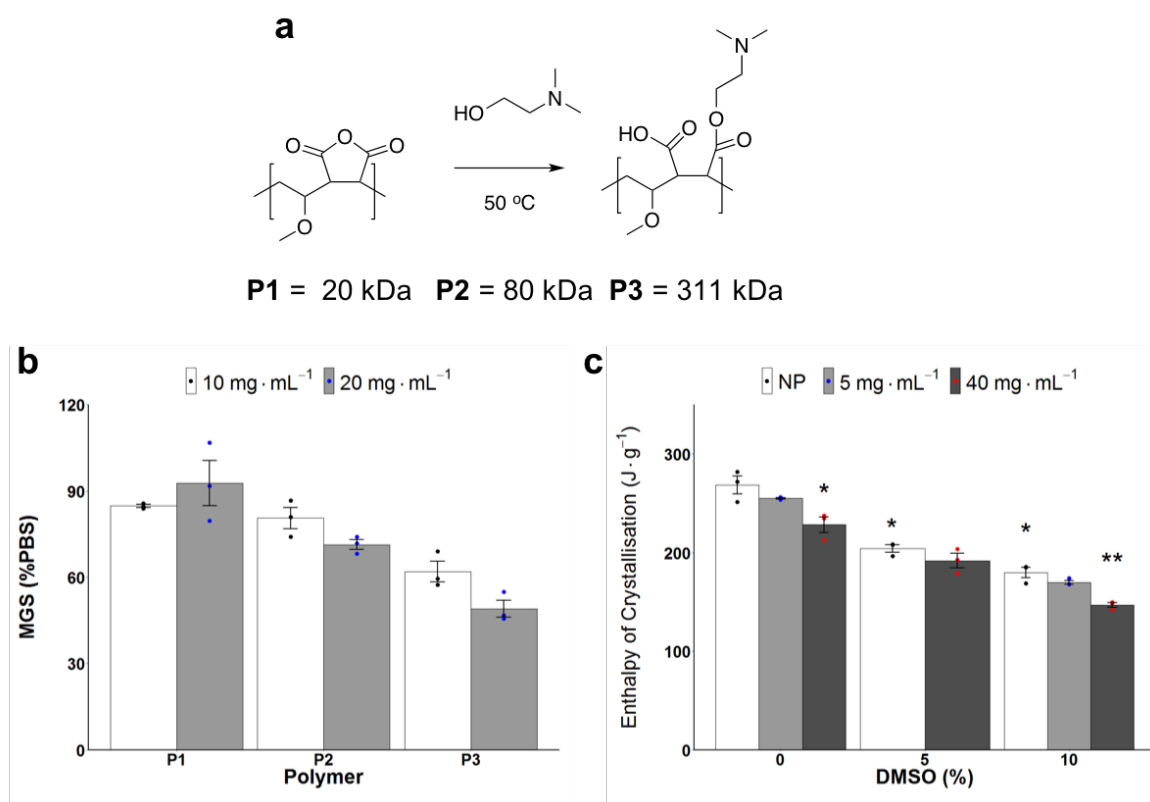


Figure 1. Polymer synthesis and ice activity. **a)** Synthesis of poly(ampholyte)s used. **b)** Ice recrystallisation inhibition assay of **P1-P3**. MGS = mean ice grain size compared to a PBS control after 30 min of annealing at $-8\text{ }^{\circ}\text{C}$. Error bars represent \pm SEM of 3 repeats. **c)** Enthalpy of crystallisation (proportional to ice volume) for cryopreservation solutions containing **P2** (NP = no polymer) via differential scanning calorimetry at a cooling rate of $1\text{ }^{\circ}\text{C}\cdot\text{min}^{-1}$. ($N = 24$, $P = 0.0000000004$, * $P < 0.001$ from NP w/0% DMSO, ** $P < 0.001$ from NP w/10% DMSO). Error bars represent \pm SEM of 3 repeats.

Erythrocyte cryopreservation was first used as a simple cellular screening model for membrane damage/stabilisation.⁴¹ Figure 2a shows that $100\text{ mg}\cdot\text{mL}^{-1}$ ($\sim 10\text{ wt}\%$) of all molecular weights

of poly(ampholytes) gave > 60 % recovery, higher than what is achieved for IRI active polymers⁴² alone (such as PVA, Figure S5) showing this unique material does not function (primarily) by ice-growth modulation. Higher concentrations could not be tested due to the solubility limits of the polymer, which is prepared at two fold concentration. The recovery levels here are comparable to those using 20 – 40 wt % glycerol, which also requires extensive post-thaw washing resulting in significant cell loss.^{28,43,44} **P2** was found to be the most potent molecular weight of cryoprotectant, giving > 80 % recovery compared to longer/shorter polymers, and erythrocytes frozen in **P2** also showed slightly less osmotic fragility than unfrozen controls (Figure S6). The post-thaw recovery values utilizing 100 mg.mL⁻¹ **P2** were also independent of pre-freeze incubation time/temperature (Figure 2b), in stark contrast to glycerol, which needs carefully controlled addition/removal to reduce toxicity and maximise recovery and introduces processing challenges which are overcome in this polymeric system.^{45,46} It should be noted that addition of uncharged water soluble macromolecules often reduces post-thaw haemolysis for erythrocytes (such as glycerol and PVP (Figure S5)), and the key aim here was to ensure the material was suitable for cryopreservation and these results were utilized for primary screening to ensure compatibility before progressing to nucleated cells (below).

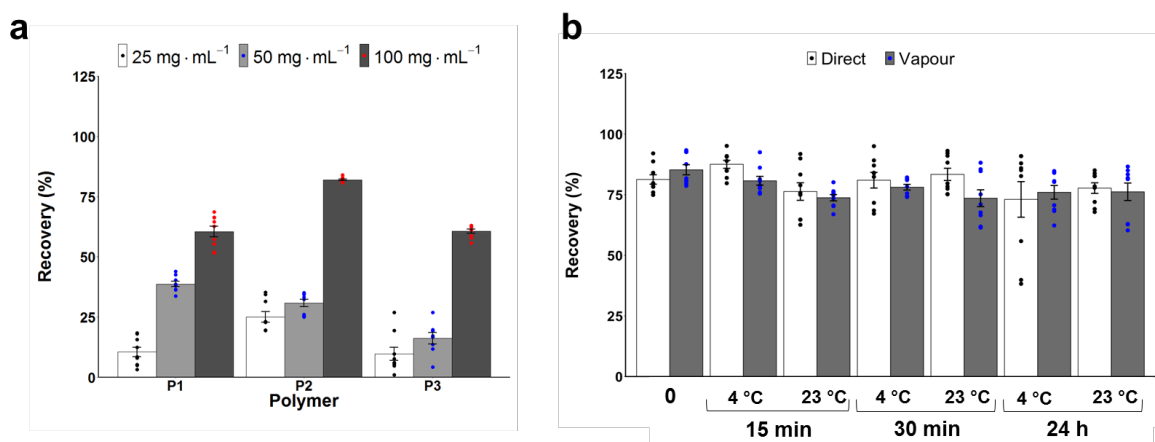


Figure 2. Red blood cell post-thaw recovery [defined as (1-haemolysis(*100))] with cryoprotective polymers. a) RBC frozen rapidly to – 196 °C/thaw 45 °C. b) Effect of pre-

freezing incubation time and temperature on post-thaw recovery with 100 mg.mL⁻¹ **P2**. Incubation time (0, 15 min, 30 min, 24 h), incubation temperature (4 °C or 23 °C), freezing conditions (directly submerged (direct) or in vapour (vapour) of liq. N₂). All error bars represent ± SEM from a minimum of 3 repeats.

Mammalian cell monolayer freezing is significantly more challenging than suspension freezing¹³ but is important for regenerative medicine, biotechnology, and basic research applications and was hence chosen as a robust challenge.⁴⁷ Confluent monolayers of A549 (epithelial lung carcinoma) cells were selected to screen for cryopreservation, using the polymer as a supplement to DMSO to increase recovery, which is already low (see data below). A549 cells were cryopreserved at 1 °C.min⁻¹ to – 80 °C, following a 10 min incubation with 10 wt % DMSO containing a concentration gradient of **P2** or PVA. PVA was used as it is a potent IRI and has been reported to enhance cell recovery by inhibiting ice recrystallisation and hence enables us to compare the utility of this new material but also mechanisms of action, as **P2** is not a potent IRI.⁴⁸ The cells were subsequently thawed, allowed to recover for 24 h, and the total cell yield determined (Figure 3b). [Note: it is crucial to allow 24 h post-thaw incubation as shorter periods give false positive results and over-estimate cell recovery.¹³] The addition of 40 mg.mL⁻¹ **P2** resulted in > 4 fold increase in recovered cells (89 %) compared to DMSO alone (20 %). Lower concentrations of **P2** also gave significant cell recovery with just 1 mg.mL⁻¹ giving a 2.5 fold increase, which is remarkable for such a dilute additive and outperforms other cryopreservative polymers.^{30–32} PVA, which has been shown to protect cells in solution during cryopreservation,²⁹ was less effect in the preservation of monolayers. Cells frozen in cryovials are in a large quantity of solution, which may make IRI activity the most important damaging factor, whereas cells frozen as monolayers exist in only a small liquid layer, therefore the benefit of IRI may not be sufficient for the protection of monolayers. These

results support our hypothesis that **P2** is a unique polymer cryoprotectant which surpasses the performance of previously reported materials and may function by a unique mechanism. Molecular weight effects of the polymer were also screened, with **P2** found to outperform **P1** and **P3** in this cryopreservation system, but all can be considered very potent cryoprotectants (Figure 3c).

Two additional mammalian cell lines, Neuro-2a and MC-3T3, were also explored. DMSO cryopreservation alone gave < 20 % cell recovery, as these cells appear more delicate than the (robust) A549 line and avenues to fine-tune the recoveries of these cells exist, as it may simply be the osmolarity for these formulations is too high, as hyperosmotic stress has been implicated in cell cycle arrest, DNA damage, oxidative stress, inhibition of transcription and translation, and mitochondrial depolarization⁴⁹ and is a known consequence of cryopreservation.⁵⁰ However, supplementing **P2** gave a 3-fold enhancement in post-thaw cell recovery in both cases (Figure 3d), showing that more fragile cells will also respond well to this new cryoprotectant. We summarise the fold-increase in post-thaw recovery compared to 10 % DMSO alone for all the cell lines in Figure 3E, demonstrating the universal applicability of our new material.

Cytotoxicity testing of **P2** revealed no decrease in cell viability for short exposure times, which are used in our cryopreservation protocol (as excess solution is removed before freezing) and were all less cytotoxic than DMSO (Figure 3f). A 24 h incubation, as a means of extreme stress outside our protocol, was conducted to exaggerate any effects and to provide mechanistic insight. Above 20 mg.mL⁻¹, 24 h incubation reduced cell metabolism and microscopy suggested membrane perturbations for long exposure times (Supp Info, Figure S7) which guided further investigations into how these polymers function (*vide infra*).

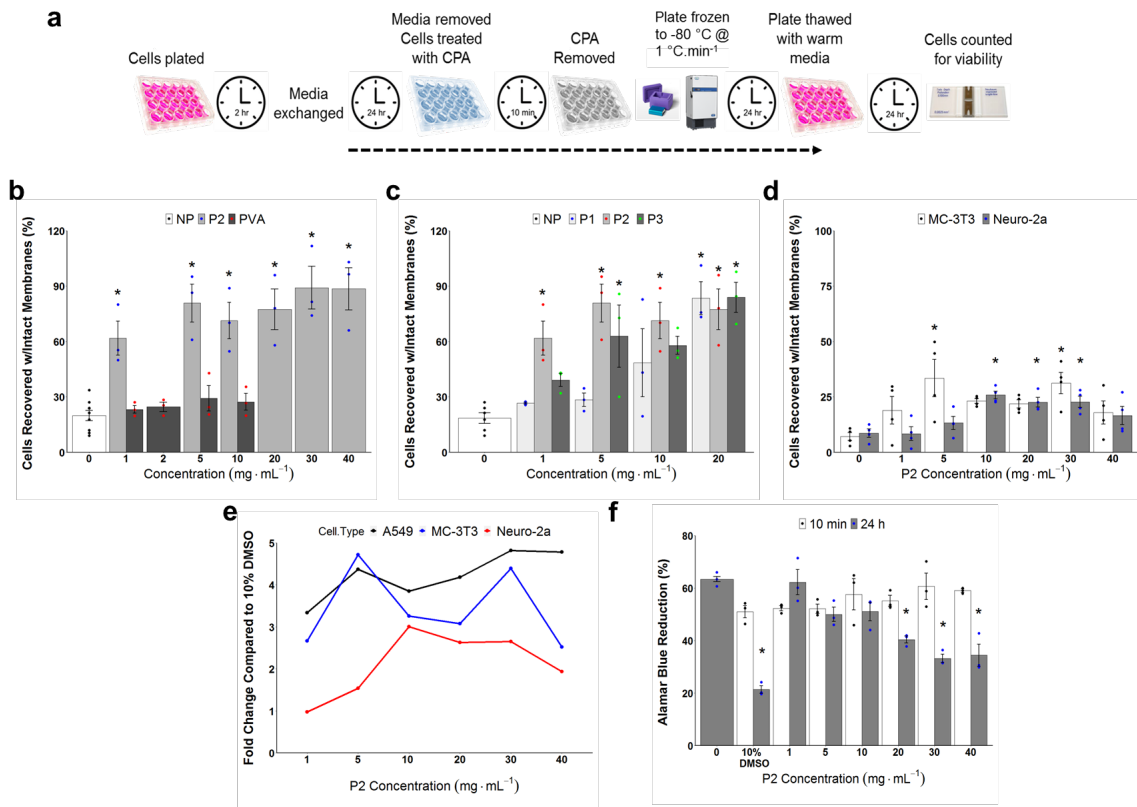


Figure 3. Cell monolayer cryopreservation and cytotoxicity. Recovered cells counted by trypan blue exclusion assay relative to unfrozen controls. All cells cryopreserved for 24 h at $-80\text{ }^{\circ}\text{C}$, then 24 h post-thaw incubation. **a)** Schematic of cryopreservation/thawing protocol; **b)** Post-thaw cell recovery (as % of unfrozen controls) of A549 cells cryopreserved with 10 % DMSO plus variable concentrations of **P2** or PVA (NP = no polymer) ($N = 39$, $P = 0.000000002$, * $P < 0.001$ from NP w/10% DMSO). The data represent the mean \pm SEM of 3 independent experiments with 2 nested replicates each. **c)** Effect of polymer molecular weight (**P1** – **P3**, NP = no polymer) and concentration on A549 cell recovery ($N = 42$, $P = 0.000006$, * $P < 0.001$ from NP w/10% DMSO). The data represent the mean \pm SEM of 3 independent experiments with 2 nested replicates each. **d)** Post-thaw recovery of Neuro-2a and MC-3T3 cells after cryopreservation with 10 % DMSO plus variable concentrations of **P2**. The data represent the mean \pm SEM of 4 independent experiments with 2 nested replicates each (Neuro-2a: $N = 28$, $P = 0.0005$, * $P < 0.001$ from Neuro-2a w/0 $\text{mg}\cdot\text{mL}^{-1}$ **P2**; MC-3T3: $N = 28$, $P = 0.02$, * $P < 0.01$ from MC-3T3 w/0 $\text{mg}\cdot\text{mL}^{-1}$ **P2**). **e)** Fold (relative to 10 % DMSO) post-thaw

recovery for all cell lines as a function of **P2** concentration. **f)** Cytotoxicity of **P2** against A549 cells, incubation time is 10 min or 24 h ($N = 48$, $P = 0.0000000001$, * $P < 0.001$ from 0 mg.mL⁻¹ **P2**). The data represent the mean \pm SEM of 3 independent experiments.

In addition to the (major) challenge of cell monolayer freezing, suspension cryopreservation is also challenging for cells that cannot tolerate the high (10 wt %) concentrations of DMSO, which has been shown to cause downstream toxicity after just 30 min of exposure (Figure S8). We therefore explored if **P2** could rescue post-thaw cell recovery when used at DMSO concentrations which are normally too low to enable cryopreservation. A549 suspension freezing showed that supplementing **P2** to 10 wt % DMSO did not enhance recovery of suspension cells, suggesting a ceiling for total recovery and distinct to the monolayer results (highlighting the challenge of cryopreservation). However, adding 20 mg.mL⁻¹ **P2** allowed DMSO reduction down to 5 wt %, and even 2.5 wt %, with cell recovery levels being comparable to 10 wt % DMSO with no polymer (Figure 4a). The ability to lower DMSO to 2.5 %, with the addition of **P2**, and retain recoveries similar to 10 wt % DMSO is a remarkable finding and will permit the cryopreservation of cells incapable of tolerating high concentrations of DMSO. Additionally, the ability to drastically lower DMSO could permit higher recoveries and allow, for example, a larger amount of human peripheral blood progenitor cells to be infused to patients.⁵¹ For A549 cells frozen as monolayers, we found that 40 mg.mL⁻¹ **P2** provided significant cell recovery at 5 wt % DMSO, demonstrating the potent cryopreservative properties of this macromolecular polymer. It was also observed that a reduction in DMSO to 5 wt %, combined with 5 mg.mL⁻¹ **P2** enabled recovery similar to polymer-free 10 % DMSO and also comparable to even lower DMSO at 2 wt % with 40 mg.mL⁻¹ **P2** (Figure 4b). The importance of this cannot be understated as lowering DMSO (whilst retaining cell yield) will dramatically increase the availability of cells for regenerative medicine, reduce downstream

toxicology challenges, and enable the storage of cells which cannot tolerate higher DMSO. For comparison, other poly(ampholytes) reported for cryopreservation required a complex, high organic solvent content solution of 6.5M ethylene glycol (~ 40 wt %), 0.5 M sucrose (~ 15 wt %) as well as 10 wt % of polymer to obtain a similar result³² or only gave cell yields below that of DMSO alone,⁵² highlighting the unique potency of the present system.

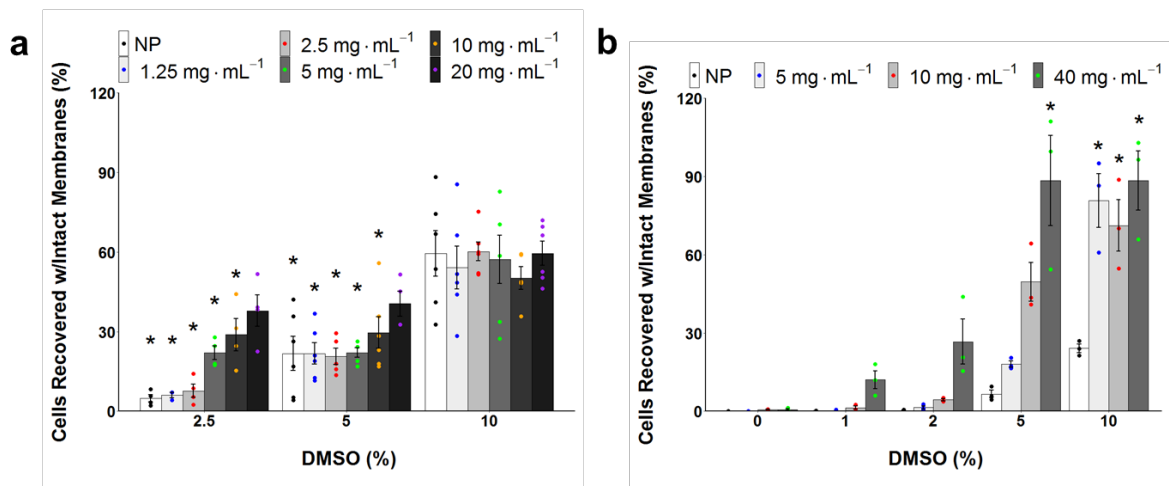


Figure 4. A549 variable DMSO/P2 suspension and monolayer cryopreservation. Recovered cells counted by trypan blue exclusion assay relative to unfrozen controls. Suspension cells cryopreserved for 24 h at $-196\text{ }^{\circ}\text{C}$, monolayer cells cryopreserved for 24 h at $-80\text{ }^{\circ}\text{C}$, both methods incubated 24 h post-thaw. **a)** Impact on suspension post-thaw recovery of varying DMSO and **P2** concentrations (NP = no polymer) ($N = 90$, $P = 0.0000000001$, * $P < 0.001$ from NP w/10% DMSO). The data represent the mean \pm SEM of at least 3 independent experiments. **b)** Impact on monolayer post-thaw recovery of varying DMSO and **P2** concentrations (NP = no polymer) ($N = 60$, $P = 0.0000000001$, * $P < 0.001$ from NP w/10% DMSO). The data represent the mean \pm SEM of 3 independent experiments with 2 nested replicates each.

While membrane integrity post-thaw is a general measure of cell survival, it does not provide any insight into long-term damage. Thus a 6 day growth assay was conducted to evaluate cell function. Post-thaw proliferation rates of A549 cells, which had been cryopreserved in a monolayer format with/without **P2**, were measured and compared to unfrozen control cells seeded at an identical density (Figure 5a). Cells cryopreserved with 10 mg.mL⁻¹ **P2** recovered at equal or faster rates than those in 10 % DMSO alone, but 40 mg.mL⁻¹ gave slower growth rates than 10 mg.mL⁻¹. Therefore, 10 mg.mL⁻¹ can be considered the optimum formulation for this format and cell line to ensure high yield and retention of function. As membrane interaction and stabilization is a potential mechanism of action, supported by the erythrocyte observations (Supp Info, Figure S6), membrane permeation post-thaw was also assessed. The ethidium homodimer-1 (EthD-1)/calcein-AM stains (LIVE/DEAD assay) were used. Healthy cells internalize calcein-AM and convert it to calcein, which then fluoresces green; EthD-1 passes through damaged membranes to nuclei where it brightly fluoresces red. Cells previously cryopreserved in 10 % DMSO had significant numbers of compromised membranes, but in contrast, addition of **P2** lead to far fewer red nuclei, supporting the hypothesis that **P2** stabilizes the cell membranes during freeze/thaw cycles (Figure 5b), graphical values are shown in Figure S9. Poly(ampholytes) are known to interact with model phospholipid membranes to a greater extent than other zwitterions such as poly(sulfobetaines)⁴⁰ and we have shown that poly(ampholyte)s do not offer any stabilization to prokaryotes which have markedly different phospholipid compositions, supporting a specific membrane interaction.⁵³

To visualize uptake or cell binding, a rhodamine 6G tagged poly(ampholyte) (confirmed in Figure S10) was synthesized and exposed to A549 cells for both 10 min and 24 h. Confocal microscopy revealed no polymer-associated intracellular or extracellularly-bound fluorescence (Figure 5c) after a single washing step and hence the unique mode of action of this polymer is purely extracellular, although not through ice interactions, unlike previous polymer

cryoprotectants.^{28,48} It is extremely beneficial that the polymer appears to be removed by simple washing, rather than multiple washings and/or equilibrations required for DMSO or glycerol (for RBCs), which is a major issue in the logistics of cell-based therapies.

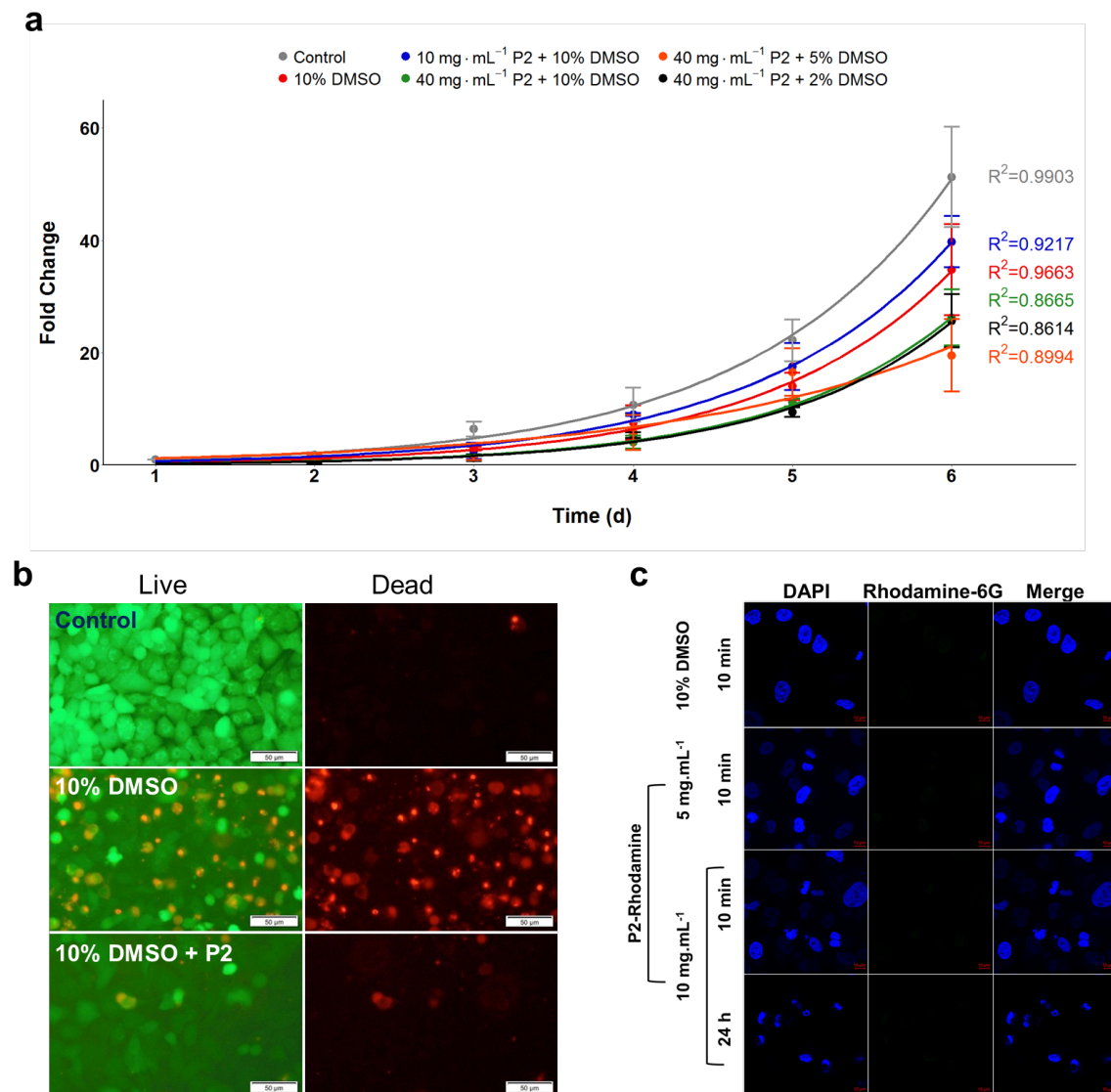


Figure 5. Post-thaw growth and polymer interaction. a) Post-thaw cell proliferation for 6 d, cells were seeded at $1.25 \cdot 10^4$ cells per well. b) LIVE/DEAD staining of A549 cells, 24 h post-thaw after cryopreservation using indicated cryoprotectants. Scale bar = 50 μm . c) Confocal fluorescence microscopy of A549 cells incubated with 10% DMSO or **P2** (with no DMSO) for indicated time and concentration. Nuclei are stained with DAPI, and incubated with **P2** tagged with rhodamine 6G, which is green fluorescent. Scale bar = 10 μm .

To further probe the impact of the polymers on membrane integrity, a membrane flux assay was modified from Su *et al.*³⁵ A549 cells were loaded with calcein-AM and the quencher trypan blue was exogenously added, allowing membrane flux to be continuously monitored by a reduction in calcein-associated fluorescence (Figure 6a). DMSO at 20 wt % (above cryopreservation levels as a positive control) led to significantly more calcein loss compared to other solutions, while DMSO at 10 wt % showed no reduction in flux, supporting the hypothesis that 10 wt % thins membranes while 20 wt % promotes pore formation,⁵⁴ yet it still remains that 10 wt % DMSO reduces cell metabolism after only 30 min at RT (Figure S8). However, all other formulations did not dramatically change the rate of flux and **P2** even lead to small reduction in flux rate at higher concentrations, supporting the membrane stabilisation hypothesis. Under identical conditions, the LIVE/DEAD stain was again applied to A549 monolayers (not frozen). After 24 h with **P2**, there were no significant changes in red nuclei at 5 mg.mL⁻¹ and only a small increase at 10 mg.mL⁻¹ (Figure 6c), but these time periods are far longer than our actual exposure time of 10 min (which is used in the pre-cryopreservation incubation protocol). Taken together this data supports a mechanism of external polymer membrane integrity stabilisation during the freezing process that enables cells to recover and proliferate faster.

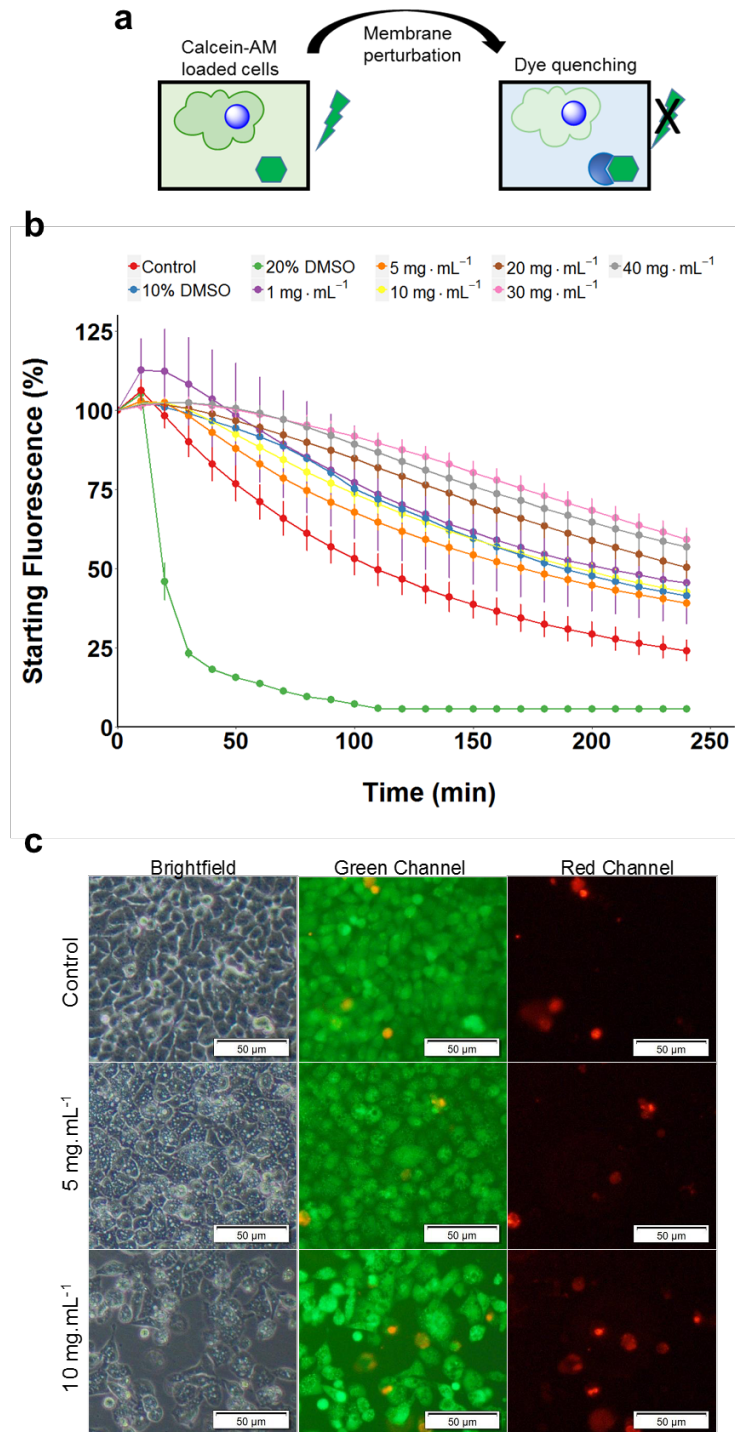


Figure 6. Impact of polymer on membrane flux and permeability. a) Graphical depiction of dye leakage assay. **b)** Continuous live cell dye leakage assay from calcein-AM loaded A549 cells treated with varying concentrations of **P2**. Decreasing fluorescence corresponds to increased membrane flux. **b)** LIVE/DEAD staining of A549 cells after 24 h incubation with **P2**. Scale bar = 50 μm .

Discussion

The cryopreservation of cells is an incredibly complex process where biochemical, as well as mechanical and physical factors, govern both the total cell recovery and the retention of function/viability. The recovery of large numbers of cells, with retention of function, is essential in cell-based therapies (to ensure therapeutic outcome) and in basic biomedical research (where cell-studies guide new treatments and understanding). Here we introduce a unique macromolecular cryopreservative which enables cells to be frozen in a monolayer format with high recovery, allows a reduction in the concentration of DMSO required for suspension and monolayer cell cryopreservation, increases the viability of recovered cells, and reduces the extent of membrane damage. This macromolecular cryopreservative, a poly(ampholyte), was obtained in a single step from a clinically used commodity bulk polymer in quantitative yield. Previous reports of polymer cryopreservatives have focused on materials which can mimic antifreeze proteins^{55,56} by controlling ice crystal formation and/or growth, which benefits cell cryopreservation.²⁸ The poly(ampholyte) we introduce here had very moderate effects on ice crystal growth, but lead to remarkable increases in post-thaw viability of over 400 % compared to DMSO alone for cell monolayers and allowed [DMSO] to be reduced to just 2 % in some cases. It was found that an 80 kDa polymer weight was optimal (**P2**), although all molecular weights were extremely potent. Mechanistic studies showed that this polymer does not enter the cells and appears to function at the membrane, stabilising it during freezing but without promoting pore formation or affecting the intrinsic membrane flux. This is supported by erythrocyte (red blood cell) studies, which are a useful model for membrane damage/stabilisation as well as a crucial component of modern medicine. Utilizing the optimal polymer, > 80 % post-thaw recovery of RBCs was possible using the polymer alone, with no additional solvents, comparable to the gold standard of glycerol,⁴⁴ but with the advantage of less processing challenges and easy removal, as it is not cell permeable. Taken

together, this data supports a mechanism where this new macromolecular cryoprotectant appears to stabilise cell membranes against cooling without affecting flux inside to outside the cell, enabling faster post-thaw recovery with more intact membranes, and fast proliferation rates. Increasing cell yields will speed up biomedical research (by reducing thaw to assay time), as well as decrease the number of donor cells required for cell-based therapies by ensuring higher recovery from the critical step of cryopreservation. Simpler and/or more effective cryopreservatives may also improve the cold chain, leading to reductions in cost associated with cell based therapies and regenerative medicine.

Conclusion

We have shown our potent and easily scalable regio-regular poly(ampholyte) significantly improves post-thaw cell recoveries of up to 88 % for adherent cell monolayers compared to just 24 % using conventional DMSO cryopreservation. The poly(ampholyte) also enables reduction of [DMSO] from 10 wt % to just 2.5 wt % in suspension cryopreservation with comparable outcomes, which can enable the preservation of DMSO-intolerant cell lines. We have also shown that this polymer leads to cells with reduced membrane damage, faster post-thaw growth rates, and can additionally cryopreserve red blood cells. Our polyampholyte appears to function extracellularly and is thus non-penetrating and easily removed. This new polyampholytic cryoprotectant will improve applications across basic and translational biomedical science and may drastically enhance the cold-chain processes for biological materials.

Author Contributions

TLB conducted mammalian cell experiments. CS undertook polymer synthesis. CS and LO undertook erythrocyte screening data. KM conducted suspension mammalian cell freezing and

DMSO toxicity. RT conducted confocal microscopy. MIG devised experiments alongside other authors and directed the research. All authors contributed to writing the manuscript.

Acknowledgements

This work was supported by the ERC (638661 and 789182 to MIG). Studentship for RT is supported by EPSRC Centre for Doctoral Training in Molecular Analytical Science, (EP/L015307/1RT). We thank the support from a seed grant through the Wellcome Warwick Quantitative Biomedicine Programme (Institutional Strategic Support Fund: 105627/Z/14/Z). The Wellcome Trust-Warwick QBP program is thanked for financial support. UoW Advanced BioImaging RTP is supported by BBSRC ALERT14 Award BB/M01228X/1. TLB thanks M. Menze for providing the Biocision CoolCell to enable controlled rate freezing.

Declarations

TLB, CS, and MIG are named inventors on a patent application relating to this work.

Supporting Information

Additional methods: osmotic fragility, Nile red staining, confocal polyampholyte uptake, neutral red staining. Additional data: polymer characterization, example splat images, DSC traces, onset melting temperatures, blood freezing with other protective compounds, osmotic fragility, mammalian cell phenotype, DMSO toxicity, graphical representation of live/dead staining post-freeze, and confirmation of rhodamine-6G tagged **P2**.

References

- (1) Wald, M. Blood Industry Shrinks as Transfusions Decline. *New York Times* **2014**.
- (2) García-Roa, M.; Del Carmen Vicente-Ayuso, M.; Bobes, A. M.; Pedraza, A. C.;

- González-Fernández, A.; Martín, M. P.; Sáez, I.; Seghatchian, J.; Gutiérrez, L. Red Blood Cell Storage Time & Transfusion: Current Practice, Concerns & Future Perspectives. *Blood Transfus.* **2017**, *15* (3), 222–231.
<https://doi.org/10.2450/2017.0345-16>.
- (3) Walsh, G. Biopharmaceutical Benchmarks 2006. *Nat. Biotechnol.* **2006**, *24* (7), 769–776. <https://doi.org/10.1038/nbt0706-769>.
- (4) Seth, G. Freezing Mammalian Cells for Production of Biopharmaceuticals. *Methods* **2012**, *56* (3), 424–431. <https://doi.org/10.1016/j.ymeth.2011.12.008>.
- (5) Kang, J.; Hsu, C. H.; Wu, Q.; Liu, S.; Coster, A. D.; Posner, B. A.; Altschuler, S. J.; Wu, L. F. Improving Drug Discovery with High-Content Phenotypic Screens by Systematic Selection of Reporter Cell Lines. *Nat. Biotechnol.* **2016**, *34* (1), 70–77. <https://doi.org/10.1038/nbt.3419>.
- (6) Karlsson, J. O. M.; Toner, M. Long-Term Storage of Tissues by Cryopreservation: Critical Issues. *Biomaterials* **1996**, *17* (3), 243–256. [https://doi.org/10.1016/0142-9612\(96\)85562-1](https://doi.org/10.1016/0142-9612(96)85562-1).
- (7) Wang, S.; Elliott, G. D. Synergistic Development of Biochips and Cell Preservation Methodologies: A Tale of Converging Technologies. *Curr. stem cell reports* **2017**, *3* (1), 45–53. <https://doi.org/10.1007/s40778-017-0074-8>.
- (8) Stéphane, X.; Najimi, M.; Sokal, E. M. Hepatocyte Cryopreservation: Is It Time to Change the Strategy? *World J. Gastroenterol.* **2010**, *16* (1), 1–14. <https://doi.org/10.3748/wjg.v16.i1.1>.
- (9) Mazur, P. Cryobiology: The Freezing of Biological Systems. *Science* **1970**, *168* (3934), 939–949. <https://doi.org/10.1126/science.168.3934.939>.
- (10) Mazur, P.; Farrant, J.; Leibo, S. P.; Chu, E. H. Survival of Hamster Tissue Culture Cells after Freezing and Thawing. Interactions between Protective Solutes and Cooling

- and Warming Rates. *Cryobiology* **1969**, *6* (1), 1–9.
- (11) Timm, M.; Saaby, L.; Moesby, L.; Hansen, E. W. Considerations Regarding Use of Solvents in in Vitro Cell Based Assays. *Cytotechnology* **2013**, *65* (5), 887–894. <https://doi.org/10.1007/s10616-012-9530-6>.
- (12) Xu, X.; Cowley, S.; Flaim, C. J.; James, W.; Seymour, L.; Cui, Z. The Roles of Apoptotic Pathways in the Low Recovery Rate after Cryopreservation of Dissociated Human Embryonic Stem Cells. *Biotechnol. Prog.* **2010**, *26* (3), 827–837. <https://doi.org/10.1002/btpr.368>.
- (13) Heng, B. C.; Ye, C. P.; Liu, H.; Toh, W. S.; Rufaihah, A. J.; Yang, Z.; Bay, B. H.; Ge, Z.; Ouyang, H. W.; Lee, E. H.; Cao, T. Loss of Viability during Freeze-Thaw of Intact and Adherent Human Embryonic Stem Cells with Conventional Slow-Cooling Protocols Is Predominantly Due to Apoptosis Rather than Cellular Necrosis. *J. Biomed. Sci.* **2006**, *13* (3), 433–445. <https://doi.org/10.1007/s11373-005-9051-9>.
- (14) Bailey, T. L.; Wang, M.; Solocinski, J.; Nathan, B. P.; Chakraborty, N.; Menze, M. A. Protective Effects of Osmolytes in Cryopreserving Adherent Neuroblastoma (Neuro-2a) Cells. *Cryobiology* **2015**, *71* (3), 472–480. <https://doi.org/10.1016/j.cryobiol.2015.08.015>.
- (15) Clark, M. S.; Thorne, M. A.; Purać, J.; Burns, G.; Hillyard, G.; Popović, Z. D.; Grubor-Lajsić, G.; Worland, M. R. Surviving the Cold: Molecular Analyses of Insect Cryoprotective Dehydration in the Arctic Springtail *Megaphorura Arctica* (Tullberg). *BMC Genomics* **2009**, *10* (1), 328. <https://doi.org/10.1186/1471-2164-10-328>.
- (16) Clegg, J. S. Metabolic Studies of Cryobiosis in Encysted Embryos of *Artemia Salina*. *Comp. Biochem. Physiol.* **1967**, *20* (3), 801–809. [https://doi.org/10.1016/0010-406X\(67\)90054-0](https://doi.org/10.1016/0010-406X(67)90054-0).
- (17) Erkut, C.; Penkov, S.; Fahmy, K.; Kurzchalia, T. V. How Worms Survive Desiccation:

- Trehalose pro Water. *Worm* **2012**, *1* (1), 61–65. <https://doi.org/10.4161/worm.19040>.
- (18) Burg, M. B. Molecular Basis of Osmotic Regulation. *Am.J Physiol* **1995**, *268* (6 Pt 2), F983–F996. <https://doi.org/10.1152/ajprenal.1995.268.6.F983>.
- (19) Armstrong, D. A.; Strange, K.; Crowe, J. H.; Knight, A.; Simmons, M. High Salinity Acclimation by the Prawn *Macrobrachium Rosenbergtii*: Uptake of Exogenous Ammonia and Changes in Endogenous Nitrogen Compounds. *Biol. Bull.* **1981**, *160* (3), 349–365. <https://doi.org/10.2307/1540844>.
- (20) Takagi, H.; Sakai, K.; Morida, K.; Nakamori, S. Proline Accumulation by Mutation or Disruption of the Proline Oxidase Gene Improves Resistance to Freezing and Desiccation Stresses in *Saccharomyces Cerevisiae*. *FEMS Microbiol. Lett.* **2000**, *184* (1), 103–108. [https://doi.org/10.1016/S0378-1097\(00\)00023-9](https://doi.org/10.1016/S0378-1097(00)00023-9).
- (21) Grothe, S.; Krogsrud, R. L.; McClellan, D. J.; Milner, J. L.; Wood, J. M. Proline Transport and Osmotic Stress Response in *Escherichia Coli* K-12. *J. Bacteriol.* **1986**, *166* (1), 253–259.
- (22) Petrenko, Y. A.; Jones, D. R. E.; Petrenko, A. Y. Cryopreservation of Human Fetal Liver Hematopoietic Stem/Progenitor Cells Using Sucrose as an Additive to the Cryoprotective Medium. *Cryobiology* **2008**, *57* (3), 195–200. <https://doi.org/10.1016/j.cryobiol.2008.08.003>.
- (23) Capicciotti, C. J.; Malay, D.; Ben, R. N. Ice Recrystallization Inhibitors: From Biological Antifreeze to Small Molecules. *Recent Dev. Study Recryst.* **2013**, 177–224. <https://doi.org/http://dx.doi.org/10.5772/54992>.
- (24) Griffith, M.; Yaish, M. W. F. Antifreeze Proteins in Overwintering Plants: A Tale of Two Activities. *Trends Plant Sci.* **2004**, *9* (8), 399–405. <https://doi.org/10.1016/j.tplants.2004.06.007>.
- (25) Moore, D. S.; Hand, S. C. Cryopreservation of Lipid Bilayers by LEA Proteins from

- Artemia Franciscana and Trehalose. *Cryobiology* **2016**, *73* (2), 240–247.
<https://doi.org/10.1016/j.cryobiol.2016.07.003>.
- (26) Congdon, T.; Notman, R.; Gibson, M. I. Antifreeze (Glyco)Protein Mimetic Behavior of Poly(Vinyl Alcohol): Detailed Structure Ice Recrystallization Inhibition Activity Study. *Biomacromolecules* **2013**, *14* (5), 1578–1586.
<https://doi.org/10.1021/bm400217j>.
- (27) Holt, C. B. The Effect of Antifreeze Proteins and Poly(Vinyl Alcohol) on the Nucleation of Ice: A Preliminary Study. *Cryo Letters* **2003**, *24* (5), 323–330.
- (28) Deller, R. C.; Vatish, M.; Mitchell, D. A.; Gibson, M. I. Synthetic Polymers Enable Non-Vitreous Cellular Cryopreservation by Reducing Ice Crystal Growth during Thawing. *Nat. Commun.* **2014**, *5*, 3244. <https://doi.org/10.1038/ncomms4244>.
- (29) Deller, R. C.; Vatish, M.; Mitchell, D. A.; Gibson, M. I. Synthetic Polymers Enable Non-Vitreous Cellular Cryopreservation by Reducing Ice Crystal Growth during Thawing. *Nat. Commun.* **2014**, *5*, 1–7. <https://doi.org/10.1038/ncomms4244>.
- (30) Graham, B.; Bailey, T. L.; Healey, J. R. J.; Marcellini, M.; Deville, S.; Gibson, M. I. Polyproline as a Minimal Antifreeze Protein Mimic That Enhances the Cryopreservation of Cell Monolayers. *Angew. Chem. Int. Ed. Engl.* **2017**, *56* (50), 15941–15944. <https://doi.org/10.1002/anie.201706703>.
- (31) Matsumura, K.; Bae, J. Y.; Kim, H. H.; Hyon, S. H. Effective Vitrification of Human Induced Pluripotent Stem Cells Using Carboxylated ϵ -Poly-L-Lysine. *Cryobiology* **2011**, *63* (2), 76–83. <https://doi.org/10.1016/j.cryobiol.2011.05.003>.
- (32) Matsumura, K.; Kawamoto, K.; Takeuchi, M.; Yoshimura, S.; Tanaka, D.; Hyon, S. H. Cryopreservation of a Two-Dimensional Monolayer Using a Slow Vitrification Method with Polyampholyte to Inhibit Ice Crystal Formation. *ACS Biomater. Sci. Eng.* **2016**, *2* (6), 1023–1029. <https://doi.org/10.1021/acsbiomaterials.6b00150>.

- (33) Matsumura, K.; Hyon, S. H. Polyampholytes as Low Toxic Efficient Cryoprotective Agents with Antifreeze Protein Properties. *Biomaterials* **2009**, *30* (27), 4842–4849. <https://doi.org/10.1016/j.biomaterials.2009.05.025>.
- (34) Stubbs, C.; Lipecki, J.; Gibson, M. I. Regioregular Alternating Polyampholytes Have Enhanced Biomimetic Ice Recrystallization Activity Compared to Random Copolymers and the Role of Side Chain versus Main Chain Hydrophobicity. *Biomacromolecules* **2017**, *18* (1), 295–302. <https://doi.org/10.1021/acs.biomac.6b01691>.
- (35) Su, M.; He, C.; West, C. A.; Mentzer, S. J. Cytolytic Peptides Induce Biphasic Permeability Changes in Mammalian Cell Membranes. *J. Immunol. Methods* **2001**, *252* (1–2), 63–71. [https://doi.org/10.1016/S0022-1759\(01\)00334-9](https://doi.org/10.1016/S0022-1759(01)00334-9).
- (36) European Food Safety Authority (EFSA), Parma, I. Scientific Opinion on the Safety of “Methyl Vinyl Ether-Maleic Anhydride Copolymer” (Chewing Gum Base Ingredient) as a Novel Food Ingredient. *EFSA J.* **2013**, *11* (3423), 1–17. <https://doi.org/10.2903/j.efsa.2013.3423>.
- (37) Knight, C. A.; Hallett, J.; DeVries, A. L. Solute Effects on Ice Recrystallization: An Assessment Technique. *Cryobiology* **1988**, *25* (1), 55–60. [https://doi.org/10.1016/0011-2240\(88\)90020-X](https://doi.org/10.1016/0011-2240(88)90020-X).
- (38) Mitchell, D. E.; Lilliman, M.; Spain, S. G.; Gibson, M. I. Quantitative Study on the Antifreeze Protein Mimetic Ice Growth Inhibition Properties of Poly(Ampholytes) Derived from Vinyl-Based Polymers. *Biomater. Sci.* **2014**, *2* (12), 1787–1795. <https://doi.org/10.1039/c4bm00153b>.
- (39) Fullerton, G. D.; Keener, C. R.; Cameron, I. L. Correction for Solute/Solvent Interaction Extends Accurate Freezing Point Depression Theory to High Concentration Range. *J. Biochem. Biophys. Methods* **1994**, *29* (3–4), 217–235.

- (40) Rajan, R.; Hayashi, F.; Nagashima, T.; Matsumura, K. Toward a Molecular Understanding of the Mechanism of Cryopreservation by Polyampholytes: Cell Membrane Interactions and Hydrophobicity. *Biomacromolecules* **2016**, *17* (5), 1882–1893. <https://doi.org/10.1021/acs.biomac.6b00343>.
- (41) Mohandas, N.; Gallagher, P. G. Red Cell Membrane: Past, Present, and Future. *Blood* **2008**, *112* (10), 3939–3948. <https://doi.org/10.1182/blood-2008-07-161166>.
- (42) Biggs, C. I.; Stubbs, C.; Graham, B.; Fayter, A. E. R.; Hasan, M.; Gibson, M. I. Mimicking the Ice Recrystallization Activity of Biological Antifreezes. When Is a New Polymer “Active”? *Macromol. Biosci.* **2019**, *1900082*, 1–9. <https://doi.org/10.1002/mabi.201900082>.
- (43) Valeri, C. R.; Ragno, G.; Pivacek, L. E.; Cassidy, G. P.; Srey, R.; Hansson-Wicher, M.; Leavy, M. E. An Experiment with Glycerol-Frozen Red Blood Cells Stored at -80°C for up to 37 Years. *Vox Sang.* **2003**, *79* (3), 168–174. <https://doi.org/doi:10.1046/j.1423-0410.2000.7930168.x>.
- (44) Briard, J. G.; Poisson, J. S.; Turner, T. R.; Capicciotti, C. J.; Acker, J. P.; Ben, R. N. Small Molecule Ice Recrystallization Inhibitors Mitigate Red Blood Cell Lysis during Freezing, Transient Warming and Thawing. *Sci. Rep.* **2016**, *6* (1), 23619. <https://doi.org/10.1038/srep23619>.
- (45) Fahy, G. M. The Relevance of Cryoprotectant “Toxicity” to Cryobiology. *Cryobiology* **1986**, *23* (1), 1–13.
- (46) Meryman, H. T.; Hornblower, M. A Method for Freezing and Washing Red Blood Cells Using a High Glycerol Concentration. *Transfusion* **1972**, *12* (3), 145–156.
- (47) Fowler, A.; Toner, M. Cryo-Injury and Biopreservation. *Ann. N. Y. Acad. Sci.* **2005**, *1066*, 119–135. <https://doi.org/10.1196/annals.1363.010>.
- (48) Deller, R. C.; Pessin, J. E.; Vatish, M.; Mitchell, D. A.; Gibson, M. I. Enhanced Non-

- Vitreous Cryopreservation of Immortalized and Primary Cells by Ice-Growth Inhibiting Polymers. *Biomater. Sci.* **2016**, *4* (7), 1079–1084.
<https://doi.org/10.1039/c6bm00129g>.
- (49) Burg, M. B.; Ferraris, J. D.; Dmitrieva, N. I. Cellular Response to Hyperosmotic Stresses. *Physiol. Rev.* **2007**, *87* (4), 1441–1474.
<https://doi.org/10.1152/physrev.00056.2006>.
- (50) Mazur, P.; Leibo, S. P.; Chu, E. H. Y. A Two-Factor Hypothesis of Freezing Injury. Evidence from Chinese Hamster Tissue-Culture Cells. *Exp. Cell Res.* **1972**, *71* (2), 345–355. [https://doi.org/10.1016/0014-4827\(72\)90303-5](https://doi.org/10.1016/0014-4827(72)90303-5).
- (51) Abrahamsen, J. F.; Bakken, A. M.; Bruserud, Ø. Cryopreserving Human Peripheral Blood Progenitor Cells with 5-Percent Rather than 10-Percent DMSO Results in Less Apoptosis and Necrosis in CD34+ Cells. *Transfusion* **2002**, *42* (12), 1573–1580.
<https://doi.org/10.1046/j.1537-2995.2002.00242.x>.
- (52) Zhao, J.; Johnson, M. A.; Fisher, R.; Burke, N. A. D.; Stöver, H. D. H. Synthetic Polyampholytes as Macromolecular Cryoprotective Agents. *Langmuir* **2019**, *35* (5), 1807–1817. <https://doi.org/10.1021/acs.langmuir.8b01602>.
- (53) Hasan, M.; Fayter, A. E. R.; Gibson, M. I. Ice Recrystallization Inhibiting Polymers Enable Glycerol-Free Cryopreservation of Microorganisms. *Biomacromolecules* **2018**, *19* (8), 3371–3376. <https://doi.org/10.1021/acs.biomac.8b00660>.
- (54) Gurtovenko, A. A.; Anwar, J. Modulating the Structure and Properties of Cell Membranes: The Molecular Mechanism of Action of Dimethyl Sulfoxide. *J. Phys. Chem. B* **2007**, *111* (35), 10453–10460. <https://doi.org/10.1021/jp073113e>.
- (55) Voets, I. K. From Ice-Binding Proteins to Bio-Inspired Antifreeze Materials. *Soft Matter* **2017**, *13* (28), 4808–4823. <https://doi.org/10.1039/C6SM02867E>.
- (56) Biggs, C. I.; Bailey, T. L.; Graham, B.; Stubbs, C.; Fayter, A.; Gibson, M. I. Polymer

Mimics of Biomacromolecular Antifreezes. *Nat. Commun.* **2017**, 8 (1).

<https://doi.org/10.1038/s41467-017-01421-7>.